27/28th International Conference
ENGINEERING MECHANICS 2022
Milovy, Czech Republic, May 9 –12, 2022
Paper **#19**, pp. 57–60, doi: 10.21495/51-2-57

WIND TUNNEL TEST OF W-WING AEROELASTIC DEMONSTRATOR

Čečrdle J.[*], Malínek P.[**], Vích O.[***]

Abstract: *This paper discusses the accomplishments in the testing of the W-WING whirl flutter demonstrator. First, the paper outlines the theoretical background on the whirl flutter phenomenon and information about the demonstrator itself, past design and development activities and preparatory experiments. The main focus is on the wind tunnel measurements. First and second experimental campaigns are described. The wind tunnel test description includes the test equipment and methodology as well as the test result assessment methodology and examples of the results. Finally, the outcome and future activities are outlined.*

Keywords: Aeroelasticity, Whirl Flutter, Aeroelastic experiment, W-WING demonstrator.

1. Introduction

Whirl flutter is a specific kind of aeroelastic flutter instability, which may appear on turboprop aircraft. Rotating mass of a propeller and a gas turbine engine rotor generates additional forces and moments and also causes aerodynamic interference effect. The instability, which is driven by motion-induced unsteady aerodynamic propeller forces and moments acting in the propeller plane, may cause unstable vibration, which can lead to a failure of an engine installation or a whole wing (Donham and Watts, 1997). The complicated physical principle of the whirl flutter requires the experimental validation of the analytically gained results, especially due to the unreliable analytical solution of the propeller aerodynamic forces. Further, a structural damping is a key parameter, to which whirl flutter is extremely sensitive and which needs to be validated. Therefore, the aeroelastic models are used. This paper is focused on the achievements in the W-WING whirl flutter demonstrator wind tunnel testing.

2. Theoretical Background

The principle is outlined on the mechanical system with two degrees-of-freedom, where an engine flexible mounting is represented by two rotational springs (stiffness K_Ψ, K_Θ), while a propeller is considered rigid (Houbolt and Reed, 1962). This system has two independent mode shapes (yaw and pitch) with angular frequencies ω_Ψ and ω_Θ. A propeller rotation (angular velocity Ω) causes both independent mode shapes merge into the whirl motion. A propeller axis shows an elliptical movement. The orientation is backward relative to the propeller rotation for the mode with the lower frequency (backward whirl mode) and forward relative to the propeller rotation for the mode with the higher frequency (forward whirl mode). The gyroscopic motion results in changes of the propeller blades' angles of attack. It causes generating of unsteady aerodynamic forces, which may under specific conditions induce whirl flutter instability. The critical flutter state is defined as the neutral stability with no damping of the system and the corresponding air velocity ($V_\infty = V_{FL}$) is called critical flutter speed. Seeking for the critical (flutter) state assuming the harmonic motion then has a character of an eigenvalue problem. The matrix equation has a following form:

$$\left(-\omega^2[M]+j\omega\left([D]+[G]+q_\infty F_P\frac{D_P^2}{V_\infty}\left[D^A\right]\right)+\left([K]+q_\infty F_P D_P\left[K^A\right]\right)\right)\begin{bmatrix}\bar{\Theta}\\ \bar{\Psi}\end{bmatrix}=\{0\} \tag{1}$$

[*] Ing. Jiří Čečrdle, Ph.D.: Czech Aerospace Research Centre (VZLU), Beranových 130; 199 05, Prague; CZ, cecrdle@vzlu.cz
[**] Ing. Petr Malínek: Czech Aerospace Research Centre (VZLU), Beranových 130; 199 05, Prague; CZ, malinek@vzlu.cz
[***] Ing. Ondřej Vích.: Czech Aerospace Research Centre (VZLU), Beranových 130; 199 05, Prague; CZ, ondrej.vich@vzlu.cz

Detailed information on the whirl flutter phenomenon may be found in Čečrdle, 2015.

3. W-WING Whirl Flutter Aeroelastic Demonstrator

"W-WING" (Whirl-Wing) is the whirl flutter demonstrator, which represents the wing (span of 2.56 m) and engine of a typical turboprop commuter aircraft. The wing and aileron stiffness is modelled by the duralumin spar, the inertial characteristics are modelled by lead weights and the aerodynamic shape is covered by the modular balsa and plastic foil segments. The nacelle model has two degrees of freedom - engine pitch and yaw. The stiffness parameters in both pitch and yaw are modelled by means of cross spring pivots with changeable spring leaves. Both pivots can be independently moved in the direction of the propeller axis to adjust the pivot points of both vibration modes. The centre of the gravity of the nacelle can be adjusted by means of the movable balance weight. The gyroscopic effect of the rotating mass is simulated by the mass of the propeller blades. Propeller is powered by an electric motor. The propeller diameter is 0.7 m. Blades' angle of attack is adjustable at the standstill. The demonstrator may be excited either by the wind flow turbulence or aerodynamically by means of the aileron deflection using various excitation signals. The detailed description on the demonstrator concept may be found in Čečrdle, Maleček and Vích, 2016.

4. Wind Tunnel Test

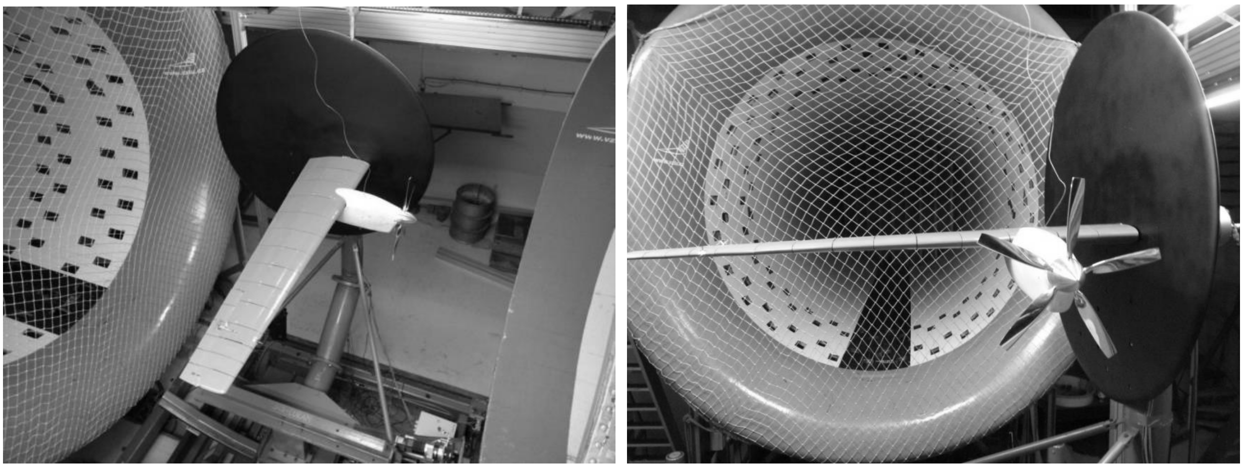

Fig. 1: Wind tunnel test arrangement.

The model is equipped with strain gauges in the wing root and half-span sections to measure the vertical bending, in-plane bending and torsional deformations. In addition, the demonstrator is also equipped with pairs of accelerometers at the engine front part and rear part providing the signals of pitch and yaw accelerations, and with a pair of accelerometers in the wing tip section providing signals of vertical acceleration. Finally, the propeller is equipped with the revolution-counting impulse sensor providing the motor-independent rpm signal. Measured quantities are acquired through the Real-Time unit. The engine is equipped with the servo-drive unit, which enables the propeller revolutions in the thrust mode to be maintained. The aileron actuation is realised via the push-pull rod by an electro-dynamic shaker. The measurement circuit is controlled by an in-house software tool. The program provides control of the propeller rotation in the thrust mode and also controls the excitation by the aileron. The program also provides the data acquisition and the selected quantities are shown in real-time. The immediate motor power and propeller revolutions are used to evaluate the propeller torque, which is the criterion for estimation of the necessity of re-adjusting the propeller blades to avoid the stall condition on the blades. The program is also used for calibration of sensors and provides the safety-guards, preventing the damage of any part of the model. The prevention of the aileron damage in the case of the shaker failure is based on the signal of the linear displacement sensor. The main safety-guard system is based on the preselected threshold acceleration value given by an arbitrary sensor. In the case of exceeding the threshold acceleration, the wind tunnel fan and the excitation are switched off. Apart from the LabVIEW-based system, the LMS TestLab system was used as well.

The model combined with the splitter plate is attached to the wind tunnel test section manipulator via the special attachment arm. The model in the wind tunnel test section is shown in Figure 1. For the measurement run, three scenarios are applicable: 1) fixed-airflow and variable-revolutions scenario, 2) fixed-revolutions and variable-airflow scenario and 3) the windmilling propeller scenario. Primary excitation was realised by the airflow turbulence only, optionally the aerodynamic excitation by the aileron flapping was used.

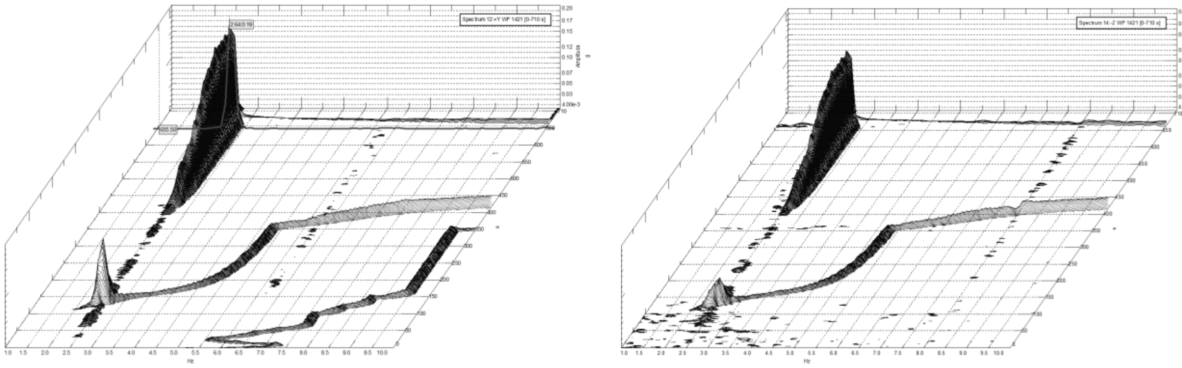

Fig. 2: Vibration spectra cascade diagrams indicating whirl frequency component growth, excitation turbulence, engine front section, flutter state reached, a) pitch, b) yaw.

The detailed assessment of result data was performed afterwards. Vibration records were processed using FFT. First, the spectra were assessed in the broad frequency range. The detailed assessment in the frequency domain was then focused on the frequency range, in which the whirl flutter was predicted. The complete result information included the airflow velocity, propeller rotational speed and the corresponding vibration spectra of all measured points over the measurement period. Next, the instant vibration spectra for each airflow velocity were evaluated, and the FFT analysis was performed at particular airflow velocities. Further, the averaged cross-power and auto-power spectra of vibrations were evaluated at the measured points and the operational modal analysis (OMA) was performed in a narrow frequency range around the expected whirl frequencies and the frequencies, mode shapes, and damping ratios were evaluated as a function of the airflow velocity and the propeller rotational speed.

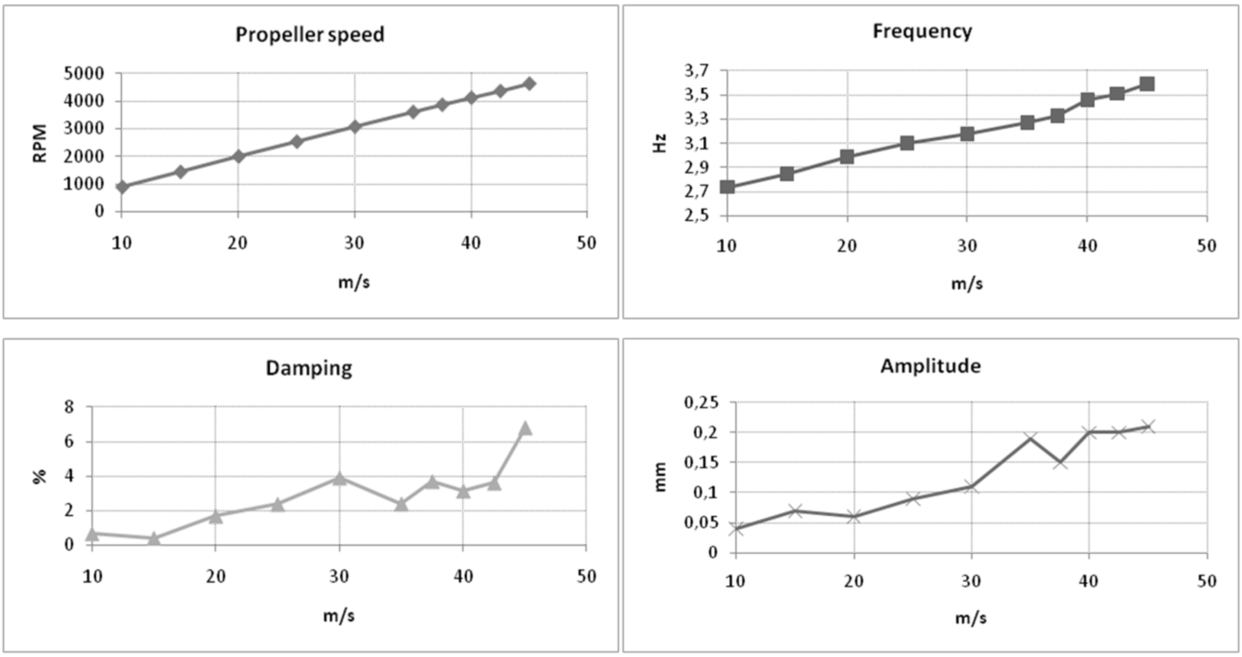

Fig. 3: Whirl mode parameters, stable case.

Two experimental campaigns have been accomplished so far. The first campaign was focused on the variation of the engine stiffness parameters (four variants), the variation of the pitch hinge station (two variants) and the variation of the balance weight station (three variants). The second experimental campaign was focused on the variation of secondary parameters. The engine stiffness remained at the configuration, for which the maximal level of vibration response has been found during the first campaign. Variable parameters included the choice of propeller (two variants), blade angle of attack (four variants), pitch hinge station (two variants) and the balance weight station (three variants).

Figure 2 shows the typical vibration spectra cascade diagrams indicating whirl frequency component growth of the measurement as the flutter is approached and finally reached. The higher level vibrations are in the pitch direction, in which the flutter amplitude threshold has also been reached. In addition, the trace of the propeller (in the windmilling mode) rotation and the crossing of the propeller rotational frequency with the pitch and yaw resonance frequencies can be found in the figures.

Figure 3 and 4 show the evaluated parameters of the whirl mode, which are shown as a function of the airflow velocity. These parameters are as follows: 1) propeller revolutions, 2) damping of the whirl mode, 3) frequency of the whirl mode and, 4) the maximal amplitude (pitch or yaw) of the engine front section. The first example (figure 3) demonstrates a very stable case, in which the amplitude of vibration is very low and the damping increases with the airflow velocity. Figure 4 shows the case, in which the instability was reached. The amplitude rapidly increases near the flutter velocity and the damping reaches zero. Note that the damping values shown in the figure were given by OMA since the values given using the logarithmic decrement (small negative values) would not be noticeable in the figures. Obviously, the unstable states with higher negative damping could not be reached due to the safety reasons.

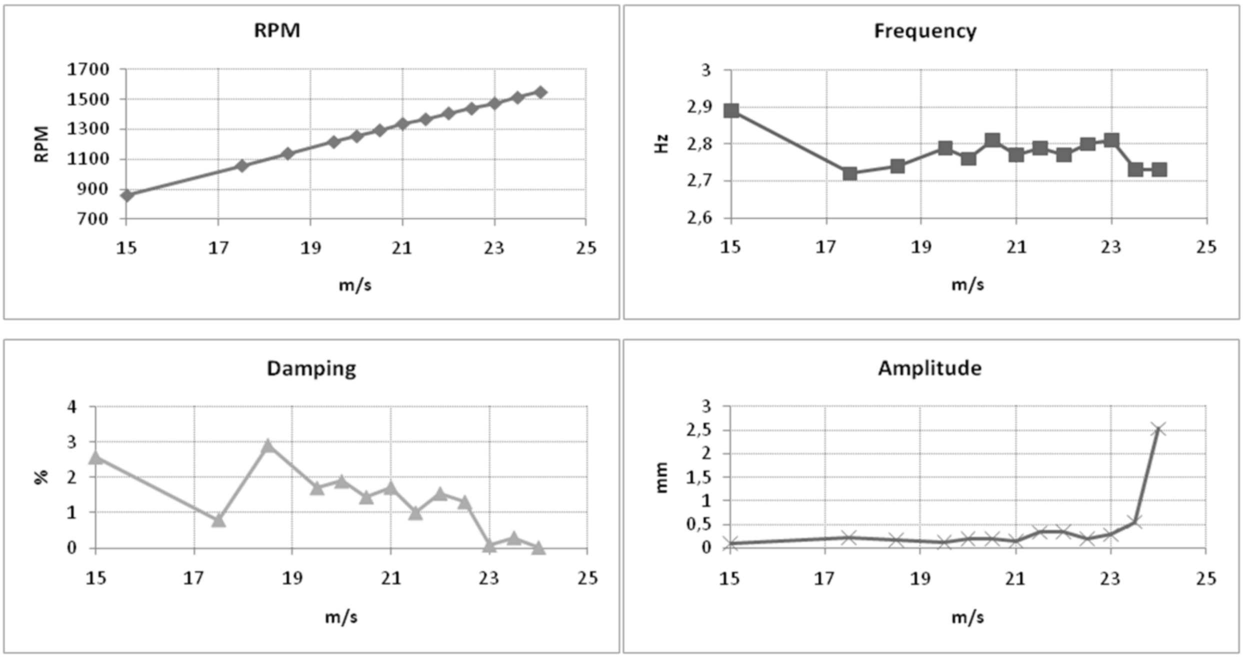

Fig. 4: Whirl mode parameters, unstable case.

5. Conclusion

The described experimental activities include the first and second experimental campaign of the newly developed whirl flutter demonstrator. Although the results did not fully meet the expectations, the results provided much useful information and experience. During the tests, technical and operational problems were also encountered. Both tests included measurement of 47 configurations of variable parameters. Flutter states were found for some configurations. The future planned activities include specifically redesigning the power system to enable the operation with no limitation in terms of the airflow velocity and propeller revolutions.

References

Čečrdle, J. (2015) *Whirl Flutter of Turboprop Aircraft Structures*. Elsevier Science. Oxford. UK.

Čečrdle, J., Maleček, J. and Vích. O. (2016) Mconcept of whirl flutter aeroelastic demonstrator. In: Zolotarev, I. and Radolf, V., eds, *Engineering Mechanics 2016*. Institute of Thermomechanics, CAS, Prague, pp.118-121.

Donham, R.E. and Watts, G.A. (1997) Whirl flutter first case. In: Flomenhoft, H., ed., *The Revolution in Structural Dynamics*, Dynaflo Press. Palm Beach Gardens. FL. USA. pp. 99-109.

Houbolt, J.C. and Reed, W.H. (1962) Propeller nacelle whirl flutter, *Journal of Aerospace Sciences*, 29, pp. 333-346.